AGU PUBLICATIONS

Geophysical Research Letters

RESEARCH LETTER
10.1002/2016GL067740

**Key Points:**
- Warm temperatures in 2013 and 2014 Australian spring are caused by stochastic climate variability
- Repeated 2013/2014 record-breaking spring temperatures unlikely without anthropogenic warming
- Likelihood of repeated recordbreaking of warm temperatures increases with anthropogenic forcing

**Supporting Information:**
- Figures S1 and S2 and Table S1

**Correspondence to:**
A. J. E. Gallant,
ailie.gallant@monash.edu

**Citation:**
Gallant, A. J. E., and S. C. Lewis (2016), Stochastic and anthropogenic influences on repeated record-breaking temperature extremes in Australian spring of 2013 and 2014, *Geophys. Res. Lett.*, *43*, 2182–2191, doi:10.1002/2016GL067740.

Received 11 JAN 2016
Accepted 12 FEB 2016
Accepted article online 15 FEB 2016
Published online 12 MAR 2016



# Stochastic and anthropogenic influences on repeated record-breaking temperature extremes in Australian spring of 2013 and 2014

**Ailie J. E. Gallant[1,2] and Sophie C. Lewis[3,2]**

[1]School of Earth, Atmosphere and Environment, Monash University, Clayton, Victoria, Australia, [2]Australian Research Council Centre of Excellence for Climate System Science, [3]Fenner School of Environment and Society, Australian National University, Acton, Australian Capital Territory, Australia

**Abstract** We examine the contribution of synoptic and interannual processes and anthropogenic warming to repeated record-breaking warmth in the Australian spring of 2013 and 2014. Climatic conditions similar to those in 2013 and 2014 have occurred in the past, the regional and large-scale interannual processes associated with these extreme temperatures were not unusual, and the repetition of the very warm temperatures is likely to be a function of stochastic interannual variability. However, analysis using observations and climate model simulations shows that without an anthropogenically driven warming trend, it is unlikely that the 2013 and 2014 temperature anomalies would have been consecutively record breaking. Climate models demonstrate that the likelihood of consecutive record-breaking spring temperatures similar to 2013 and 2014 changes from $< 1\%$ in simulations using natural forcing only to between 11% and 25% for the period 2006–2020 using simulations containing both natural and anthropogenic forcings.

## 1. Introduction

In the presence of persistent memory in a time series, for example, an underlying trend like background warming, extreme events are more likely to occur and are more likely to be clustered [*Bunde et al*., 2005], and the expected incidence of record-breaking events increases [*Ballerini and Resnick*, 1987; *Benestad*, 2003; *Wergen et al*., 2013]. Outside this statistical context, the underlying physical processes changing the incidence of extremes often remain unclear. Understanding these processes is crucial for identifying and constraining the likely behavior of future extremes in the context of an ongoing background-warming trend, for example, as a result of anthropogenic climate change [*International Panel on Climate Change*, 2013].

Record-breaking extreme heat occurring concurrently with a warming trend will be associated with either stochastic variability independent of the warming trend or one or both of the following mechanisms. The first is that the process inducing the background warming, or the warming itself, causes a change in the immediate processes causing the extreme heat, for example, strengthening land surface feedbacks [e.g., *Seneviratne et al*., 2006]. Alternatively, there might be little change to these underlying processes, but with warming these occur under a uniformly warmer air mass.

Using an Australian case study, we examine the contribution of each of these mechanisms to repeated, record-breaking heat extremes that occurred in the austral spring (September-October-November, SON) of 2013 and 2014. In 2013, a new Australian area-average seasonal mean temperature ($T_{mean}$) record (*T*2) was set for SON (Figure 1a) [*Bureau of Meteorology*, 2013; *Arblaster et al*., 2014; *Tihema*, 2014]. In 2014, the 2013 Australian spring $T_{mean}$ record was exceeded and the 2014 spring $T_{mean}$ (*T*1) became the largest positive anomaly for any season ever recorded [*Bureau of Meteorology*, 2014; *Hope et al*., 2015a, 2015b].

Aspects of the anomalously warm spring temperatures in Australia in 2013 and 2014 have been investigated previously. *Arblaster et al*. [2014] assessed the regional processes associated with these record warm temperature anomalies, and *Lewis and Karoly* [2014] used a probabilistic approach to examine the anthropogenic influence on the likelihood of the extreme heat. However, the regional and anthropogenic processes causing the consecutive nature of the 2013 and 2014 spring extremes have not been considered. Moreover, the regional processes causing the extreme temperatures have not been placed in a historical context to determine if they are a part of any long-term trend. Knowledge about the presence or absence of changes in the processes themselves is invaluable for constraining estimates of the likely occurrence of future temperature extremes.

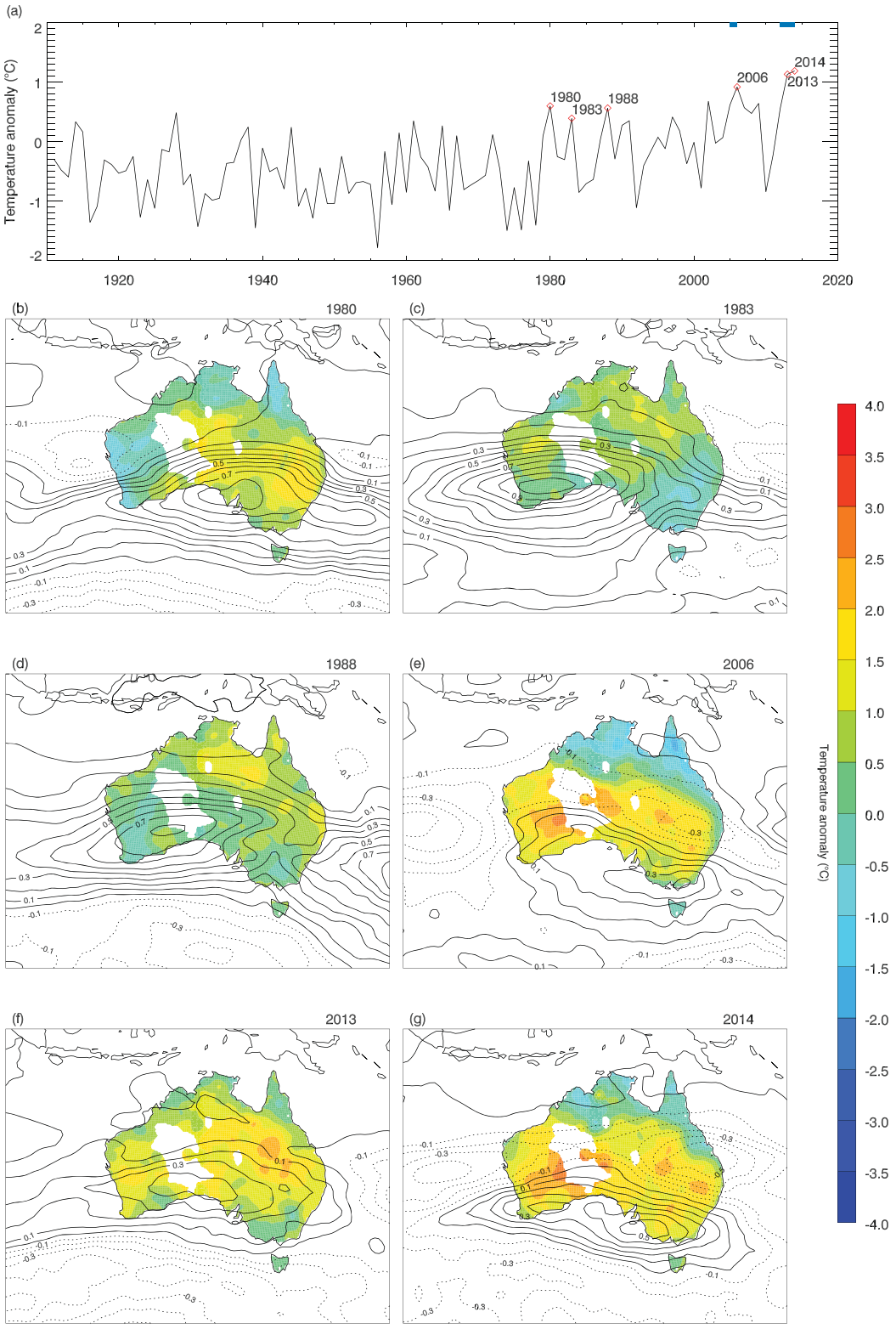


**Figure 1.** (a) Time series of the observed September-October-November (SON) Australian area-averaged $T_{mean}$ anomalies. The five warmest SON mean temperatures from detrended data are shown by the red diamonds. The blue lines on the upper *x* axis show the three warmest pairs of years. (b–g) The shading shows SON $T_{mean}$ anomalies, and the black contour lines positive (solid) and negative (dashed) SON $PV_{350}$ anomalies for 1980, 1983, 1988, 2006, 2013, and 2014, respectively. All observed $T_{mean}$ anomalies are computed relative to 1979–2010.

This study examines the underlying processes associated with repeated Australian spring temperature records. We will show that the repetition of two warm SON $T_{mean}$ anomalies in 2013 and 2014 was likely caused by stochastic interannual variability in regional-scale mechanisms, but we argue that the repetition of these events was more likely to be a result of uniform warming across regional Australia rather than systematic changes to these regional-scale processes.

## 2. Data and Methods

### 2.1. Observational Data

Observed Australian area-average SON $T_{mean}$ anomalies were calculated from the Australian Water Availability Project (AWAP) data set [*Jones et al*., 2009]. Areas lacking data prior to the 1970s are excluded from the analysis [e.g., *Gallant et al*. [2013]] (see Figures 1b–1g). As AWAP data have not been subjected to temporal homogeneity adjustments [*Fawcett et al*., 2012], we compare them with the high-quality, homogenized ACORN-SAT data set for 1910–2014 [*Trewin*, 2012] (Figure S1a in the supporting information). Differences between the two data sets in the later half of the record are nearly indistinguishable. In both data sets, 2013 is ranked as the second warmest and 2014 as the warmest SON $T_{mean}$ on record.

To determine if the 2013 and 2014 were unusual in a historical context, we examine their regional and large-scale climatic conditions compared to past years with warm SON $T_{mean}$ anomalies: 1980, 1983, 1988, and 2006 (Figures 1b–1e). These years were chosen as they had the four warmest, area-averaged warm SON $T_{mean}$ anomalies outside 2013 and 2014 in the post-1978 period when an estimate of the mean long-term warming trend was removed. Only years post-1978 were selected because the ERA-Interim data, used to examine the regional atmospheric conditions, begins in 1979. The warming trend removed from the area-averaged $T_{mean}$ time series was a fourth-order polynomial fit of the ensemble mean from historical climate model simulations (see Figure S1), making the detrending more physically realistic than using a simple statistical estimate such as linear regression. The processes relating to interannual SON $T_{mean}$ variability, described below, also employed these detrended data.

Warm temperature extremes over Australia have been linked to regional circulation patterns in the upper atmosphere [e.g., *Arblaster et al*., 2014; *Parker et al*., 2014; *Hope et al*., 2015a]. We examined this connection using potential vorticity on the 350 K potential temperature isentropic surface ($PV_{350}$). $PV_{350}$ is a quantity used for the effective examination of multiple aspects of the dynamical atmospheric circulation [*Hoskins et al*., 1985]. Monthly and daily $PV_{350}$ data were obtained from the ERA-Interim reanalysis data [*Dee et al*., 2011], and its anomalies were calculated relative to 1979–2010.

The El Niño–Southern Oscillation (ENSO) and the Southern Annular Mode (SAM) are related to anomalous warmth across Australia [*Nicholls et al*., 1996; *Hendon et al*., 2007; *Perkins et al*., 2015]. ENSO was represented by the Niño 3.4 index, defined as anomalous area-averaged sea surface temperatures, relative to 1981–2010 bounded by the domain 5°S–5°N, 120°E–170°W [*Trenberth*, 1997], which was obtained from the National Oceanic and Atmospheric Administration's Climate Prediction Center (http://www.cpc.ncep.noaa.gov/data/indices/) and was computed using Extended Reconstructed Sea Surface Temperature v3B [*Smith et al*., 2008]. Marshall's SAM index [*Marshall*, 2003] (http://www.nerc-bas.ac.uk/icd/gjma/sam.html) represented the SAM and is computed as the anomalous zonally averaged pressure difference between 45°S and 60°S using 12 stations at these latitudes. SAM anomalies were computed relative to 1971–2000 [*Marshall*, 2003].

The contribution of preceding dry conditions to the anomalous warmth of 2013 and 2014 was also examined. As soil moisture data were not yet available post-2013, area-averaged rainfall anomalies from AWAP [*Jones et al*., 2009] were applied as a proxy for surface moisture availability. Rainfall averaged over the July-August-September (JAS) period had the strongest statistical relationship ($r = -0.5$) with SON $T_{mean}$.

All statistical relationships were quantified using Pearson correlations, and the degrees of freedom for statistical significance calculations were adjusted for the presence of autocorrelations following *Bretherton et al*. [1999].

### 2.2. Model Data

We utilize Coupled Model Intercomparison Project Phase 5 (CMIP5) [*Taylor et al*., 2012] detection and attribution experiments to determine the likely contribution of anthropogenic greenhouse gas emissions

to the repeated spring temperature extremes (Table S1). The models analyzed here are identical to those used by *Lewis and Karoly* [2014] (Table S1). For SON $T_{mean}$, the historical simulations from nine CMIP5 models analyzed are statistically indistinguishable ($p = 0.05$) to the distribution of observed average temperatures over the period 1911–2005 (Figure S1b) evaluated using a two-sided Kolmogorov-Smirnov test.

Data were analyzed from the CMIP5 historical experiment, which simulates the climate of 1850–2005 with observed time-evolving forcing (imposed well-mixed greenhouse gases, tropospheric aerosols and ozone, volcanic aerosols, and solar irradiance). We also use the CMIP5 historicalNat model experiment in which subsets of known forcings (volcanics aerosols and solar irradiance) are applied. As the consecutive 2013/2014 extreme spring temperatures occurred after the historical simulation terminates in 2005, we also use the RCP (Representative Concentration Pathway) 8.5 experiment [*Peters et al*., 2012]. We consider only RCP8.5 years for the period 2006–2020, which is centered on the present. Finally, as an estimate of unforced climate variability, we examine the piControl long simulations completed for each CMIP5 model with no changes in external forcings.

Australian area-averaged SON $T_{mean}$ anomalies were calculated for the historical and historicalNat simulations relative to the 1911–1940 model climatology, the RCP8.5 anomalies from the relevant model's historical 1911–1940 climatology, and the piControl anomalies relative to the long-term mean for each ensemble member. The use of the different climatologies for the models (long-term control or 1911–1940) and observations (1979–2005) does not affect estimates of changes in the probability of extremes. All model data were regridded onto a 1.5° latitude by 1.5° longitude horizontal grid, and at least 75% of each grid box had to be composed of land surface to be included in area-average temperature calculations.

The differences in the likelihood of hot spring temperatures with and without anthropogenic forcing are explored using the fraction of attributable risk (FAR) framework. The FAR value [*Stone and Allen*, 2005] is calculated as

$$\mathrm{FAR} = 1 - \frac{P_{\mathrm{NAT}}}{P_{\mathrm{ALL}}} \tag{1}$$

where $P_{NAT}$ denotes the probability of an event occurring in a natural reference state (historicalNat) and $P_{ALL}$ under a parallel forced state (historical, RCP8.5 experiment) with both natural and anthropogenic forcing. The FAR values reported here are conservative estimates, with an assessment of uncertainty obtained by bootstrap resampling modeled temperature distributions (see supporting information).

We investigate differences in the likelihood of extreme spring temperatures occurring in single years using temperature thresholds $\Delta T1$, $\Delta T2$, $\Delta T3$, and $\Delta T4$, where $\Delta T1$ is the warmest, $\Delta T2$ is the second warmest etc temperature anomaly from the observational record. We also examine extreme SON $T_{mean}$ values occurring in 2 year periods, including the second (2012–2013, $\Delta T2_{consec}$) and third (2005–2006, $\Delta T3_{consec}$) hottest mean consecutive SON temperatures observed. By this definition, the order of the hottest and second-hottest years is inconsequential.

## 3. The Factors Contributing to the Record Warmth in 2013 and 2014

The repeated nature of the SON $T_{mean}$ records in 2013 and 2014 was unprecedented. Figures 1f and 1g show their associated anomalous climatic conditions. The warmest conditions during SON in 2013 and 2014 were in September and October, respectively. Although both years had much warmer than normal minimum temperatures, the $T_{mean}$ anomalies were mostly the result of anomalously high maximum temperatures.

### 3.1. Regional and Large-Scale Factors

The previously identified regional-scale mechanisms associated with warm SON $T_{mean}$ are preceding dry conditions [*Timbal et al*., 2002; *Arblaster et al*., 2014; *Hope et al*., 2015a], and strong, anomalous circulations [*Arblaster et al*., 2014; *Hope et al*., 2015a]. The related large-scale mechanisms are El Niño conditions and a strongly negative phase of the SAM [*Nicholls et al*., 1996; *Hendon et al*., 2007; *Arblaster et al*., 2014; *Hope et al*., 2015a]. The likely contribution of each of these factors to the 2013 and 2014 SON $T_{mean}$ anomalies, and a comparison with other warm years (1980, 1983, 1988, and 2006), is provided below. We do not examine other processes that might influence SON extreme heat, as these are difficult to identify in a chaotic climate system.

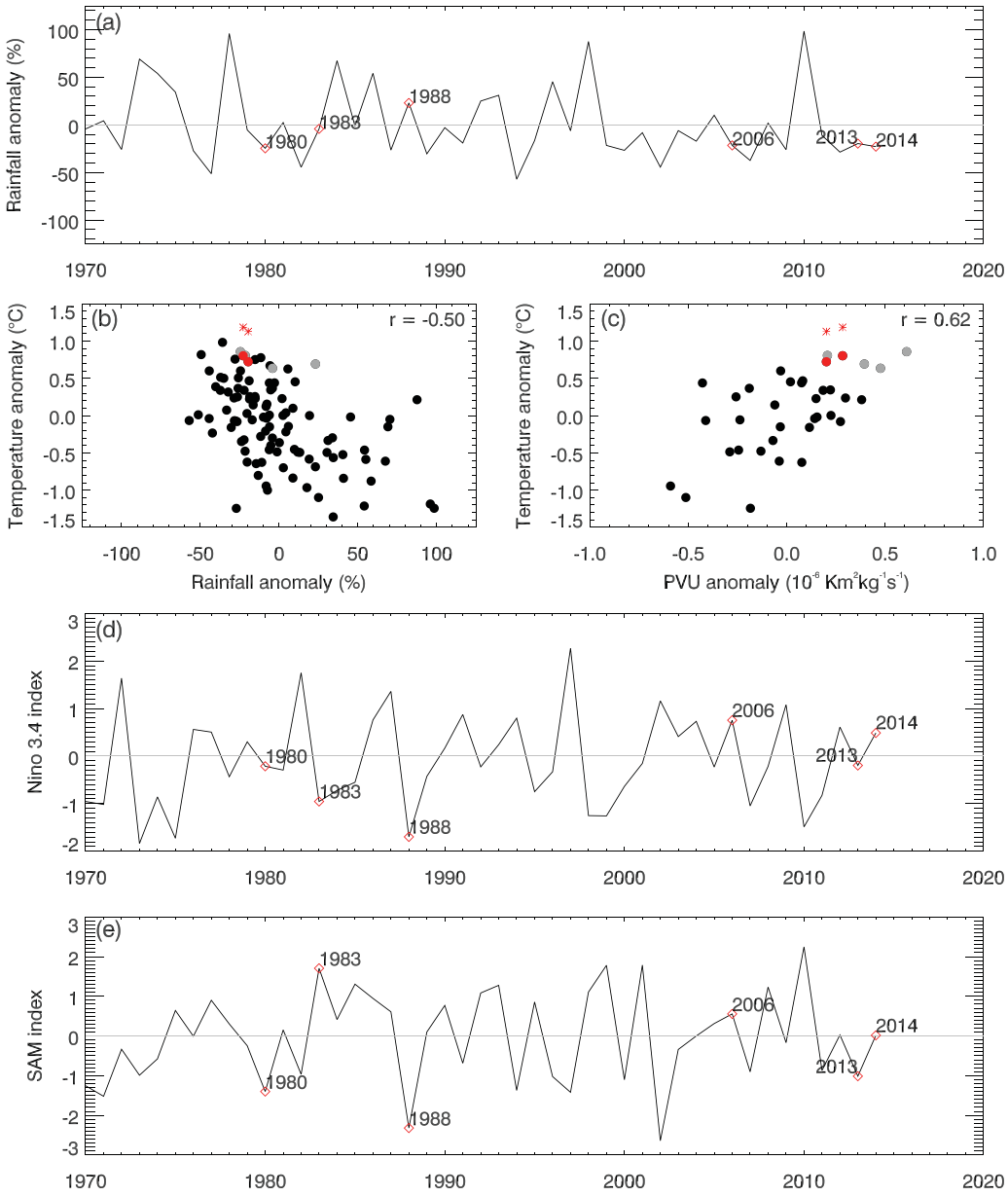


**Figure 2.** (a) Time series of the July–September Australian area-averaged Australian rainfall anomaly (%), which is representative of antecedent soil moisture conditions. The relationship between the detrended SON $T_{mean}$ anomaly and (b) JAS rainfall anomaly (%), and (c) area-averaged $PV_{350}$ anomaly bounded by the area 120°E–150°E and 30°S–40°S is shown. Here the grey dots highlight the years 1980, 1983, 1988, and 2006, and the red dots 2013 and 2014. The red crosses show the 2013 and 2014 data computed using the raw SON $T_{mean}$ anomalies, which include the long-term warming trend. (d and e) The time series of the SON Niño 3.4 index and the SON SAM index.

Using data from 1911 to 2014, JAS rainfall shares 25% of its interannual variability with SON $T_{mean}$ (90% confidence interval (CI) of 14%–38% calculated using 10,000 bootstrapped resamples). The majority of this covariability is unrelated to ENSO, with a partial variance shared between JAS rainfall and SON $T_{mean}$ with the Niño 3.4 index removed of 19% (90% CI of 6%–36%). From this statistical relationship, lower area-averaged rainfall in JAS is associated with warmer area-averaged SON $T_{mean}$ (Figure 2b). The years 2013 and 2014 were not drier than previous warm SON years, ranking 27th and 34th driest in the 1911–2014 record (Figure 2a). Therefore, it is unlikely that preceding dry conditions substantially amplified the 2013 and 2014 SON $T_{mean}$ anomalies compared to past years.

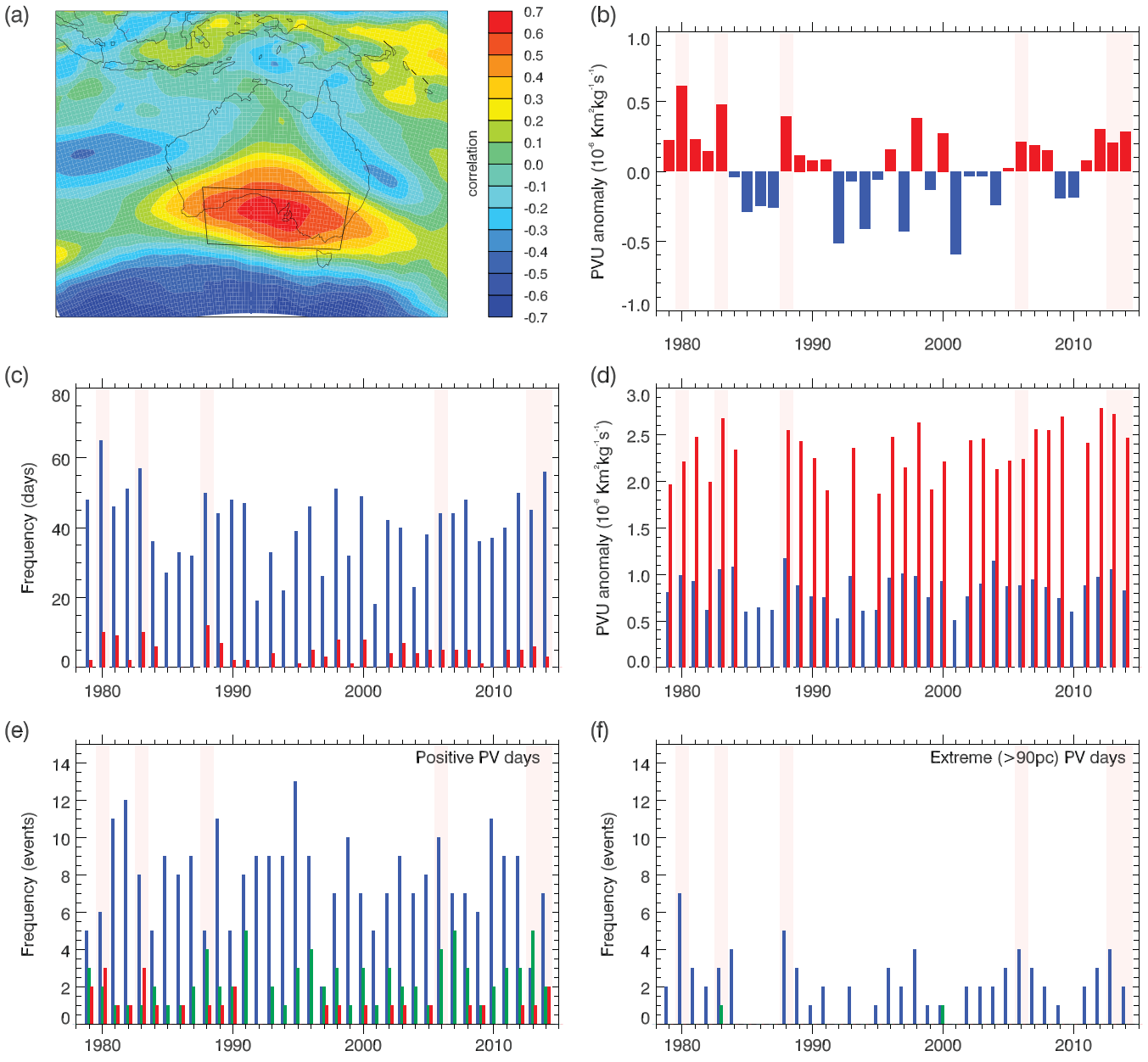


**Figure 3.** (a) The correlation between grid point $PV_{350}$ anomalies and Australian area-averaged SON $T_{mean}$ anomalies and (b) the time series of mean SON $PV_{350}$ anomaly for Southern Australia (see text for definition). (c and d) The frequency and mean magnitude, respectively, of days when the area-averaged daily $PV_{350}$ anomalies in Southern Australia are positive (blue bars) or exceed the 90th percentile, defined as extreme (red bars). (e and f) Days from Figure 3c when positive or extreme $PV_{350}$ anomalies persisted for $< 5$ days (blue), 5–9 days (green), and $\geq 10$ days (red). In Figures 3b–3f pink shading highlights the years 1980, 1983, 1988, 2006, 2013, and 2014.

Warmer than normal SON temperatures are typically associated with a strong, anticyclonic $PV_{350}$ anomaly over southern Australia (Figures 1b–1g, 2c, 3a, and S2). An area bounded by 120°E–150°E and 30°S–40°S, hereafter called Southern Australia, shows the strongest relationship (Figure 3a). Anomalies in $PV_{350}$ here share up to 46% of the interannual variations in Australian area-averaged SON $T_{mean}$ anomalies.

Warm $T_{mean}$ anomalies were largest over southern and central-east Australia in 2014 and 2013, respectively. There was a strongly anomalous upper level anticyclonic circulation over Southern Australia during both years, which is typical of past very warm SON years (Figures 1b–1g) and all much warmer than normal SONs in Australia (Figure S2). However, note that the spatial pattern of warming across the continent differs

with the location of the upper level anticyclonic anomaly. The $PV_{350}$ anomalies associated with the record-breaking warmth in 2014 and 2013 were ranked sixth and eleventh, respectively, by magnitude (Figure 3b).

Daily $PV_{350}$ anomalies reveal the characteristics of the synoptic features associated with the seasonal $PV_{350}$ anomalies (Figures 3c–3f). These characteristics highlight the contributions of frequency, magnitude, and/or persistence of the daily upper level circulation to the warm seasonal-scale $T_{mean}$ anomalies. The six warmest years show differences in the contribution of these daily-scale characteristics to the seasonal $PV_{350}$ anomaly. There were a similar number of days with positive $PV_{350}$ anomalies in 2006 and 2013; however, in 2006 most systems lasted less than 5 days. In 2013 most systems lasted 5–9 days and were associated with larger magnitude $PV_{350}$ anomalies (Figures 3d–3f). There was a high frequency and magnitude of short-lived (<5 days), positive $PV_{350}$ anomalies in 2014, but these metrics were not unprecedented (e.g., 1980) (Figures 3c–3f).

There is little evidence that the frequency, magnitude, and/or persistence in the daily $PV_{350}$ anomalies influenced the 2013 and 2014 seasonal SON $T_{mean}$ anomalies because the characteristics were not unusual compared to past years. In fact, days with upper level anticyclonic anomalies over southern Australia were generally more frequent, larger in magnitude, and/or persistent in the 1980s.

Changes to the Australian regional circulation can also arise from the large-scale influences of ENSO and the SAM. El Niño conditions are weakly related to warmer than normal area-averaged SON $T_{mean}$ ($r = 0.32$, $p < 0.01$) [*Nicholls et al.*, 1996]. However, the effect of ENSO on Australia's warmest spring temperatures is mixed, e.g., 1988 was a La Niña and 2006 an El Niño. ENSO was near neutral in 2013, and in 2014 weak El Niño conditions were present. Therefore, it is unlikely that ENSO was a strong contributor to the SON $T_{mean}$ anomalies during 2013 or 2014.

We compute a statistically significant but weak relationship between the SAM index and SON $T_{mean}$ anomalies ($r = -0.36$, $p < 0.01$). Figure 2e shows that the SAM was in a negative phase in 2013 and near neutral in 2014. The SAM typically persists for 10–20 days during the austral spring [*Baldwin et al.*, 2003], suggesting greater importance for intraseasonal, rather than seasonal-scale variability. The years 1980 and 1988 had more strongly negative SAM conditions compared to 2013 and 2014, with 1988 the second largest negative anomaly between 1979 and 2014. Therefore, if the SAM did contribute to the strength of the record-breaking temperature anomalies, it was in 2013 only. However, the comparison with 1980 and 1988 shows that it is unlikely that the SAM was responsible for the 2013 temperature anomaly being over 50% larger than the temperature anomaly of either 1980 or 1988.

Finally, the contribution of persistence of warm temperature anomalies in the winter months preceding SON was investigated. The correlations between winter and spring $T_{mean}$ were weak (maximum $r = 0.34$ in August), and none of the warmest springs also had similarly warm August mean temperatures.

Whether assessed individually or in combination, an analysis of those factors most strongly contributing to the interannual variations in SON $T_{mean}$ shows that the climatic conditions in 2013 and 2014 were not noticeably different to past years with large, positive SON $T_{mean}$ anomalies. The detrended temperature data described in section 2.1 support this and show that 2013 and 2014 are cooler than both 1980 and 2006 when the estimate of regional anthropogenic warming is removed (Figures 2b and 2c).

### 3.2. Anthropogenic Factors

The regional climatological conditions and prevailing large-scale modes of variability in SON of 2013 and 2014 do not provide a convincing explanation alone for the magnitude of the observed $T_{mean}$ anomalies when compared to other very warm years. Moreover, it is not clear whether the repeated nature of the record-breaking anomalies is coincidental. To address this gap, the role of background anthropogenic warming is now explored (Figure 4a).

The probability of hot (i.e., $> \Delta T4$) Australian SON temperatures is significantly higher in simulations that impose anthropogenic forcings than in those that do not (Figure 4b). It is very likely (>90%) that anthropogenic forcings increase the likelihood of simulated SON temperatures greater than $\Delta T4$ by at least 5 times (FAR = 0.82), although in the RCP8.5 experiments, which are most relevant to observed conditions in 2013 and 2014, hot SON temperatures are calculated as 20 times more likely (FAR = 0.95). When the 2013 ($\Delta T2$) and 2014 ($\Delta T1$) thresholds are considered, it becomes significantly less likely that model simulations reach these extreme temperatures with naturally forced climate variability alone. Such extreme $\Delta T1$ temperatures

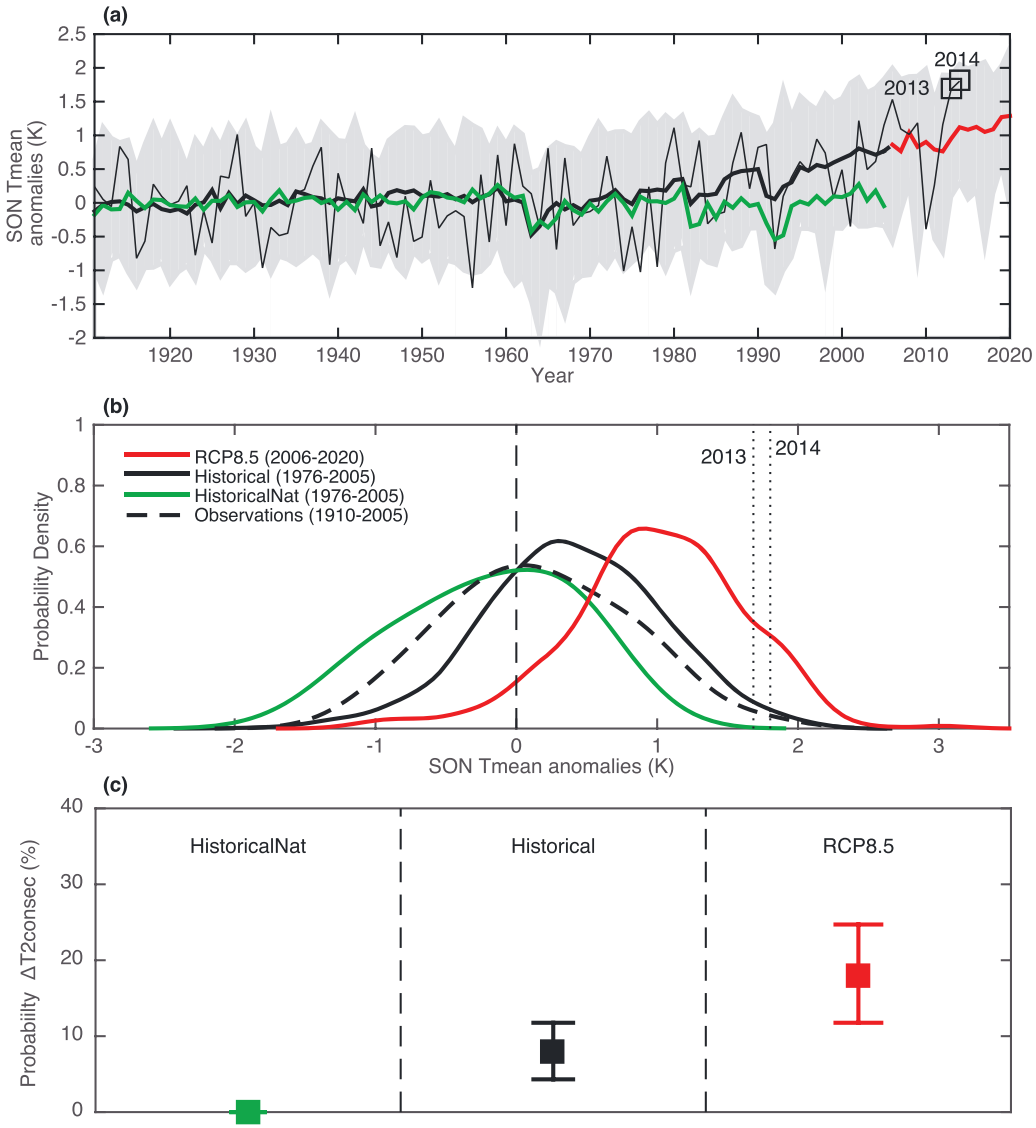


**Figure 4.** (a) Australian SON $T_{mean}$ anomalies (K) for observations (thin black), historicalNat (green), historical (black) and RCP8.5 (red) multimodel mean. The grey plume indicates the 5th–95th percentile-simulated range of SON temperatures across historical model ensemble members. (b) Probability density estimates for Australian average SON anomalies for observations (years 1910–2014, dashed black), compared with historicalNat (green, years 1976–2005), historical (black, years 1976–2005), and RCP8.5 (red, years 2006–2020). Vertical dashed lines show the observed 2013 ($\Delta T2$) and 2014 ($\Delta T1$) anomalies. (c) Probability (%) of consecutive extreme (each year $> \Delta T4$) Australian average SON $T_{mean}$ anomalies occurring in historicalNat (green, years 1976–2005), historical (black, years 1976–2005), and RCP8.5 (red, years 2006–2020) simulations.

occur in only 5 out of 8058 piControl years and in 2 out of 4992 historicalNat model years (in the full runs extending from 1850 to 2005), but in 24 out of 1950 historical years and in 47 of 525 RCP8.5 years. When the probability of $\Delta T2$ in historical simulation is compared to the historicalNat over the same years (1976–2005), such extremes are not obtained without anthropogenic forcings (i.e., FAR = 1).

The likelihood of consecutive very warm SON temperatures, such as 2013 and 2014, was compared between experiments by binning years and calculating 2 year running mean values. In this case, we calculated the FAR values for exceeding the second (2012–2013, $\Delta T2_{consec}$) and third (2005–2006, $\Delta T3_{consec}$) hottest mean consecutive SON temperatures observed. The likelihood of such hot consecutive SON temperatures occurring in the historicalNat is substantially lower than in the anthropogenically forced experiments. For the historical years 1976–2005, there is very likely a 25-fold (FAR = 0.96) increase in the risk of exceeding

$\Delta T3_{consec}$ that can be attributed to anthropogenic forcing. For the RCP8.5 years 2006–2020, it is at least 100 times more likely (FAR = 0.99). There is no period of 2 year consecutive Australian spring warmth in the piControl or historicalNat simulations as warm as that observed in 2012–2013 ($\Delta T2_{consec}$) or 2013–2014 ($\Delta T1_{consec}$).

The likelihood of consecutive spring heat was further explored in 10,000 bootstrap simulations of the temperature time series from the various model experiments, using 50% of available model years in each iteration. The chance of observing high consecutive spring temperatures, with each year greater than $\Delta T4$, was very small in the historicalNat simulations (<1%). However, it was very likely (>90% confidence) that there would be an 11% chance that any 2 year consecutive period in the RCP8.5 experiment would exceed the simulated spring temperature $\Delta T4$. That is, consecutive Australian spring heat, such as that observed in 2005–2006, 2012–2013, and 2013–2014, is significantly more likely to occur in anthropogenically forced experiments (Figure 4c). Thus, the model experiments indicate that anthropogenic warming can alter the likelihood of consecutive record-breaking events, which is an attribute of interannual climate variability [e.g., *Bunde et al*., 2005].

## 4. Summary and Conclusions

Our analysis shows that the continent-averaged extreme spring temperatures of 2013 and 2014 were likely the combined result of coincident regional and large-scale intraannual to interannual scale processes compounded by a primarily anthropogenically driven background-warming trend that elevated temperatures to record-breaking levels. Preliminary data shows SON $T_{mean}$ in 2015 ranked behind only 2014 [*Bureau of Meteorology*, 2016], which is a third consecutive year of recurrent near record-breaking anomalies.

The analysis of regional and large-scale mechanisms showed that climatic states similar to 2013 and 2014 have occurred in the past. The influence of these processes is nuanced, likely nonlinear, and there will be at least some contribution from processes not examined here. However, all past years with these similar conditions produced temperatures at least 0.21°C (0.27°C) cooler than 2013 (2014).

Evidence from climate model simulations demonstrated that it is very likely that anthropogenic forcing contributed to the repeated nature of the record breaking of the 2013 and 2014 SON $T_{mean}$ anomalies. Simulations including anthropogenic forcing increased the likelihood of repeated temperature extremes from < 1%, with natural forcing only, to between 11% and 25% for the current period (2006–2020) when both natural and anthropogenic forcings were included in the model simulations.

These results highlight that anthropogenic warming probably influenced the likelihood of the repetition of record-breaking warm spring temperatures in 2013 and 2014. We have demonstrated that this repetition is likely to be a result of background warming inducing uniformly warmer conditions, rather than a change to the underlying causal processes of the extreme heat that are occurring concurrent to background warming.

**Acknowledgments**
This research was supported by the ARC Centre of Excellence for Climate System Science (grant CE 110001028), ARC DECRAs DE150101297 and DE160100092, and the NCI National Facility. AWAP data are from the Bureau of Meteorology, the Bureau of Rural Sciences, and CSIRO and the ERA-Interim data from ECMWF. The WCRP's Working Group on Coupled Modelling is responsible for CMIP, and the U.S. Department of Energy's PCMDI provides CMIP5 coordinating support.

## References

Arblaster, J. M., E. P. Lim, H. H. Hendon, B. C. Trewin, M. C. Wheeler, G. Liu, and K. Braganza (2014), Understanding Australia's hottest September on record—[in explaining extremes of 2013 from a climate perspective], *Bull. Am. Meteorol. Soc.*, *95*, S37–S41.

Baldwin, M. P., D. B. Stephenson, D. W. J. Thompson, T. J. Dunkerton, A. J. Charlton, and A. O'Neill (2003), Stratospheric memory and skill of extended-range weather forecasts, *Science*, *301*, 636–640, doi:10.1126/science.1087143.

Ballerini, R., and S. I. Resnick (1987), Records in the presence of a linear trend, *Adv. Appl. Probab.*, *19*, 801–828, doi:10.2307/1427103.

Benestad, R. E. (2003), How often can we expect a record event?, *Clim. Res.*, *25*, 3–13, doi:10.3354/cr025003.

Bretherton, C. S., M. Widmann, V. P. Dymnikov, J. M. Wallace, and I. Blade (1999), The effective number of spatial degrees of freedom of a time-varying field, *J. Clim.*, *12*, 1990–2009.

Bunde, A., J. F. Eichner, J. W. Kantelhardt, and S. Havlin (2005), Long-term memory: A natural mechanism for the clustering of extreme events and anomalous residual times in climate records, *Phys. Rev. Lett.*, *94*, doi:10.1103/physrevlett.94.048701.

Bureau of Meteorology (2013), Australia's warmest September on record *Special Climate Statement 46*. [Available at http://www.bom.gov.au/climate/current/statements/scs46.pdf.]

Bureau of Meteorology (2014), Annual Climate Report 2013, 36 pp. [Available at http://www.bom.gov.au/climate/annual_sum/2013/index.shtml.]

Bureau of Meteorology (2016), Annual Climate Report 2015, 36 pp. [Available at http://www.bom.gov.au/climate/annual_sum/2013/index.shtml.]

Dee, D. P., et al. (2011), The ERA-Interim reanalysis: Configuration and performance of the data assimilation system, *Q. J. R. Meteorol. Soc.*, *137*, 553–597, doi:10.1002/qj.828.

Fawcett, R. J. B., B. C. Trewin, K. Braganza, R. J. Smalley, B. Jovanovic, and D. A. Jones (2012), On the sensitivity of Australian temperature trends and variability to analysis methods and observation networks *CAWCR Technical Report No. 050*, Australian Bureau of Meteorology, 66 pp.

Gallant, A. J. E., M. J. Reeder, J. S. Risbey, and K. J. Hennessy (2013), The characteristics of seasonal-scale droughts in Australia 1911–2009, *Int. J. Climatol.*, *33*, 1658–1672, doi:10.1002/joc.3540.
Hendon, H. H., D. W. J. Thompson, and M. C. Wheeler (2007), Australian rainfall and surface temperature variations associated with the Southern Hemisphere annular mode, *J. Clim.*, *20*, 2452–2467, doi:10.1175/jcli4134.1.
Hope, P., E. P. Lim, G. Wang, H. H. Hendon, and J. M. Arblaster (2015a), Contributors to the record high temperatures across Australia in late spring 2014—[in explaining extremes of 2014 from a climate perspective], *Bull. Am. Meteorol. Soc.*, *96*, S149–S153.
Hope, P., P. Reid, S. Tobin, M. Tully, A. Klekociuk, and P. Krummel (2015b), Seasonal climate summary southern hemisphere (spring 2014): El Niño continues to try to break through, and Australia has its warmest spring on record (again!), *Aust. Meteorol. Oceanogr. J.*, *65*, 267–292.
Hoskins, B. J., M. E. McIntyre, and A. W. Roberston (1985), On the use and significance of isentropic potential vorticity maps, *Q. J. R. Meteorol. Soc.*, *111*, 877–946.
International Panel on Climate Change (2013), Annex I: Atlas of global and regional climate projections, in *Climate Change 2013: The Physical Science Basis. Contribution of Working Group I to the Fifth Assessment Report of the Intergovernmental Panel on Climate Change*, edited by T. F. Stocker et al., pp. 1311–1394, Cambridge Univ. Press, Cambridge, U. K., and New York, doi:10.1017/CBO9781107415324.029.
Jones, D. A., W. Wang, and R. Fawcett (2009), High-quality spatial climate data-sets for Australia, *Aust. Meteorol. Oceanogr. J.*, *58*, 233–248.
Lewis, S. C., and D. J. Karoly (2014), The role of anthropogenic forcing in the record 2013 Australia-wide annual and spring temperatures [in explaining extremes of 2013 from a climate perspective], *Bull. Am. Meteorol. Soc.*, *95*, S31–S34.
Marshall, G. J. (2003), Trends in the southern annular mode from observations and reanalyses, *J. Clim.*, *16*, 4134–4143, doi:10.1175/1520-0442.
Nicholls, N., B. Lavery, C. Frederiksen, W. Drosdowsky, and S. Torok (1996), Recent apparent changes in relationships between the El Niño-Southern Oscillation and Australian rainfall and temperature, *Geophys. Res. Lett.*, *23*, 3357–3360, doi:10.1029/96GL03166.
Parker, T. J., G. J. Berry, and M. J. Reeder (2014), The structure and evolution of heat waves in southeastern Australia, *J. Clim.*, *27*, 5768–5785, doi:10.1175/JCLI-D-13-00740.1.
Perkins, S. E., D. Agueso, and C. J. White (2015), Relationships between climate variability, soil moisture and Australian heatwaves, *J. Geophys. Res. Atmos.*, *120*, 8144–8164, doi:10.1002/2015JD023592.
Peters, G. P., R. M. Andrew, T. Boden, J. G. Canadell, P. Ciais, C. Le Quéré, G. Marland, M. R. Raupach, and C. Wilson (2012), The challenge to keep global warming below 2°C, *Nat. Clim. Change*, *3*, 4–6, doi:10.1038/nclimate1783.
Seneviratne, S. I., D. Lüthi, M. Litschi, and C. Schär (2006), Land-atmosphere coupling and climate change in Europe, *Nature*, *443*, 205–209, doi:10.1038/nature05095.
Smith, T. M., R. W. Reynolds, T. C. Peterson, and J. Lawrimore (2008), Improvements to NOAA's historical merged land-ocean surface temperature analysis, *J. Clim.*, *21*, 2283–2296, doi:10.1175/2007jcli2100.1.
Stone, D. A., and M. R. Allen (2005), The end-to-end attribution problem: From emissions to impacts, *Clim. Change*, *71*, 303–318, doi:10.1007/s10584-005-6778-2.
Taylor, K. E., R. J. Stouffer, and G. A. Meehl (2012), An overview of CMIP5 and the experiment design, *Bull. Am. Meteorol. Soc.*, *93*, 485–498, doi:10.1175/bams-d-11-00094.1.
Tihema, T. (2014), Seasonal climate summary southern hemisphere spring (spring 2013): Warmest Australian spring on record, *Aust. Meterol. Oceanogr. J.*, *64*, 149–160.
Timbal, B., S. Power, R. Colman, J. Viviand, and S. Lirola (2002), Does soil moisture influence climate variability and predictability over Australia?, *J. Clim.*, *15*, 1230–1238, doi:10.1175/1520-0442.
Trenberth, K. E. (1997), The definition of El Niño, *Bull. Am. Meteorol. Soc.*, *78*, 2771–2777, doi:10.1175/1520-0477.
Trewin, B. (2012), A daily homogenized temperature data set for Australia, *Int. J. Climatol.*, *33*, 1510–1529, doi:10.1002/joc.3530.
Wergen, G., A. Hense, and J. Krug (2013), Record occurrence and record values in daily and monthly temperatures, *Clim. Dyn.*, *42*, 1275–1289.